

AD-A161 740

A STUDY OF SURFACE PROPERTIES OF SUPERCONDUCTING  
MATERIALS FOR HIGH POWER. (U) CALIFORNIA UNIV SAN DIEGO  
LA JOLLA INST FOR PURE AND APPLIED P. H SUHL ET AL.

1/1

UNCLASSIFIED

31 OCT 85 N00014-82-K-0578

F/G 20/3

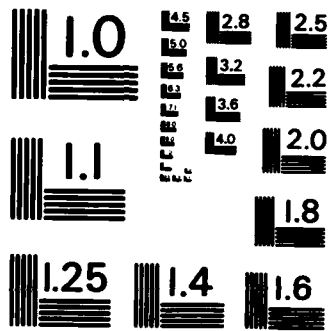
NL



END

PL

PL



MICROCOPY RESOLUTION TEST CHART  
NATIONAL BUREAU OF STANDARDS-1963-A

12

REPORT DOCUMENTATION PAGE

AD-A161 740

|   |       |  |   |
|---|-------|--|---|
| 2. REPORT SECURITY CLASSIFICATION<br><u>Unclassified</u>  |       | 1d. RESTRICTIVE MARK NGS   |   |
| 1. SECURITY CLASSIFICATION AUTHORITY  |       | 3. DISTRIBUTION/AVAILABILITY OF REPORT   |   |
| 4. DECLASSIFICATION/DOWNGRADING SCHEDULE  |       |  |   |
| PERFORMING ORGANIZATION REPORT NUMBER(S)  |       | 5. MONITORING ORGANIZATION REPORT NUMBER(S)  |   |
| 6a. NAME OF PERFORMING ORGANIZATION<br>University of California,<br>San Diego   |       | 6b. OFFICE SYMBOL<br>(If applicable)   |   |
| 7a. NAME OF MONITORING ORGANIZATION<br>ONR Resident Representative  |       |  |   |
| 8. ADDRESS (City, State and ZIP Code)<br>La Jolla, CA 92093   |       | 7b. ADDRESS (City, State and ZIP Code)<br>Mail Code Q-043<br>University of California, San Diego<br>La Jolla, CA 92093 |   |
| 6a. NAME OF FUNDING/SPONSORING ORGANIZATION<br>Office of Naval Research   |       | 6b. OFFICE SYMBOL<br>(If applicable)   |   |
| 8. PROCUREMENT INSTRUMENT IDENTIFICATION NUMBER<br>N00014-82-K-0578   |       |  |   |
| 8c. ADDRESS (City, State and ZIP Code)<br>Department of the Navy<br>800 North Quincy Street<br>Arlington, Virginia 92093  |       | 10. SOURCE OF FUNDING NOS.   |   |
| 11. TITLE (Include Security Classification)<br>See Box 16   |       | PROGRAM ELEMENT NO.  | PROJECT NO.   |
|   |       | TASK NO.   | WORK UNIT NO.   |
| 12. PERSONAL AUTHOR(S)<br>Harry Suhl and Wayne Vernon   |       |  |   |
| 13a. TYPE OF REPORT<br>Final Technical  |       | 13b. TIME COVERED<br>FROM 82Aug01 TO 85Aug31   |   |
|   |       | 14. DATE OF REPORT (Yr., Mo., Day)<br>85Oct 31   |   |
|   |       | 15. PAGE COUNT<br>5  |   |
| 16. SUPPLEMENTARY NOTATION<br>A study of Surface Properties of Superconducting Materials for High Power Microwave Applications  |       |  |   |
| 17. COSATI CODES  |       | 18. SUBJECT TERMS (Continue on reverse if necessary and identify by block number)                                      |   |
| FIELD   | GROUP | SUB. GR.   | Superconducting RF, Nb <sub>3</sub> Sn Properties, Critical Fields<br>Cavity loss mechanisms <sup>3</sup> ← |
|   |       |  |   |
|   |       |  |   |
| 19. ABSTRACT (Continue on reverse if necessary and identify by block number)<br>We have investigated electric and magnetic critical field levels for Nb and Nb <sub>3</sub> Sn superconductors. Since the maximum power levels for RF-Superconducting cavities seem to be limited by maximum magnetic field capability, most of the work involved studies of the time dependence of flux penetration into Nb <sub>3</sub> Sn samples where maximum field limits are unknown. We find that the lower critical field (H <sub>c2</sub> ) of Nb <sub>3</sub> Sn is about 600 gauss at low temperature and 2MHz frequency of applied field, but flux penetration occurs at very low level so that considerably higher field values will not lead to large power loss. Additional interesting effects are associated with Nb <sub>3</sub> Sn on Nb substrates which may also lead to increased peak power capability. |       |  |   |
| 20. DISTRIBUTION/AVAILABILITY OF ABSTRACT<br>UNCLASSIFIED/UNLIMITED <input type="checkbox"/> SAME AS RPT. <input type="checkbox"/> DTIC USERS <input type="checkbox"/>  |       | 21. ABSTRACT SECURITY CLASSIFICATION   |   |
| 22a. NAME OF RESPONSIBLE INDIVIDUAL   |       | 22b. TELEPHONE NUMBER (Include Area Code)  | 22c. OFFICE SYMBOL<br>E   |

DTIC FILE COPY

85 11 07 030

DTIC ELECTED NOV 27 1985

FINAL REPORT

A STUDY OF SURFACE PROPERTIES OF SUPERCONDUCTING  
MATERIALS FOR HIGH POWER  
MICROWAVE APPLICATION

October 31, 1985

for

Office of Naval Research  
N00014-82-K-0578  
8/1/82-8/31/85

Principal Investigators: Harry Suhl, Wayne Vernon

Institute for Pure and Applied Physical Sciences  
University of California, San Diego  
La Jolla, CA 92093



|                     |   |
|---------------------|---|
| Accession For       |   |
| NTIS                | GRA&I <input checked="" type="checkbox"/> |
| DTIC                | TAB <input type="checkbox"/>              |
| Unannounced         | <input type="checkbox"/>                  |
| Justification       | <i>per</i>                                |
| By _____            |   |
| Distribution/ _____ |   |
| Availability Codes  |   |
| Dist                | Avail and/or<br>Special                   |
| <i>A-1</i>          | -   |

The use of superconductors for high power RF has been limited by the peak electric and magnetic fields which can be achieved in cavities. We sought to explore the limitations of such devices by looking at field emission of electrons from Nb surfaces at high electric fields and by investigating magnetic field flux penetration for large peak fields at the surface. Since there seems to be no fundamental electric field limitation below 100 MV/m field strengths, most of our effort has gone into magnetic field studies. In typical cavities a peak magnetic field of 1 kilo-Gauss somewhere in the cavity corresponds to a peak electric field in the vicinity of 30 MV/m at some other location, and materials such as Nb<sub>3</sub>Sn have not been shown to have critical fields ( $H_{C1}$ ) as high as 1 kilo-Gauss. Our efforts have, therefore, moved in the direction of finding what happens to materials such as Nb<sub>3</sub>Sn when the surface begins to allow magnetic field flux penetration into the bulk of the sample.

At the beginning of the project we studied field emission with Nb samples and constant electric fields over 1 cm wide samples. A clean high vacuum system with a turbo molecular pump was used for the studies. We found that simple etching of the sample followed by glow discharge cleaning in low pressure Ar gas allowed us to obtain electric field strengths of  $\sim 40$  MV/m before discharge or high electron currents were observed. There seems to be some consensus of opinion that field emission problems in cavities can be eliminated by a combination of careful fabrication, good vacuum systems, keeping dust out and performing low pressure He or Ar discharge cleaning (especially at high power pulsed RF drive). The question of what leads to the breakdown in DC circumstances has become more difficult to understand,<sup>(1)</sup> and the study of such questions has grown in sophistication<sup>(2)</sup> to the point where our small effort was not competitive.

The next step in this three year project was the study of flux penetration into small samples of Nb and Nb<sub>3</sub>Sn when an external time varying magnetic field was imposed, initially with a ferrite gapped toroid providing

the magnetic field. Since we wished to study a variety of sample shapes, both solid and hollow, a sense scheme was devised to allow measurement of flux penetration into a sample by measuring voltages from two coils, one surrounding the sample and one which monitored the applied field. A constant fraction of the applied field sense coil voltage was subtracted from the sample coil voltage so that the difference represented a departure from linearity of the flux in the sample versus the applied field. In this way we can measure both threshold critical fields ( $H_{c1}$ ) and the magnitude of energy loss per cycle of flux penetration into the sample or other non-linear effects at the surface of the sample.

Our initial efforts were mostly concentrated on a pure  $Nb_3Sn$  crystal with external magnetic fields at frequencies below 20 kHz, a restriction due to complications in high frequency behavior of the cold ferrite being used to create the applied field. The results of these studies are shown in the appendix which is a copy of the conference paper<sup>(3)</sup> presented to the Applied Superconductivity Conference last year. It appeared that there is definitely some striking frequency dependence in the motion of flux into  $Nb_3Sn$  samples. Even though there appeared to be a rather low critical field for  $Nb_3Sn$  ( $\sim 600$  Gauss), the degree of flux penetration was rather small, even at these low frequencies. This has immediate consequences for RF applications, especially if the magnitude of flux penetration continues to drop as frequency is increased. In addition, our measurement of the lower critical field for  $Nb_3Sn$  may be a better way to determine this elusive parameter than has been achieved in the past.

The next step in this study consisted of making Helmholtz coils and associated high power drivers to permit us to reach 2 kilo-Gauss peak magnetic fields at frequencies of up to 2 MHz. At the same time we fabricated a series of samples which would be more suited to the new geometry. We chose a cylindrical shape of 1 mm dia by 4 mm length in order to eliminate end effects by keeping induced current densities at the sample surface smaller at the ends of the sample than at the middle (where the

flux monitor coil is positioned). A series of thin shell samples was prepared so that the core of the cylinder would not contain conducting material which reduces our sensitivity to observed flux penetration. The  $Nb_3Sn$  sample was fabricated by diffusing tin into Nb tubes with 0.15 mm wall thickness and resulted in high quality  $Nb_3Sn$  on the Nb substrate.

Studies of the new samples have been conducted at frequencies up to 2 MHz (which required a 5 kw pulsed RF transmitter to drive the Helmholtz coils) and some interesting effects have been seen in the behavior of the  $Nb_3Sn$  on Nb sample. There is no discernible flux penetration at the expected  $H_{c1}$  of  $Nb_3Sn$  when operating at 4.2°K, but we do see the threshold associated with Nb (~ 1.2 kG). On the other hand, when working at 10°K the expected lower  $H_{c1}$  (~ 400 Gauss) of  $Nb_3Sn$  is observed which is expected because the Nb has become "normal." The thickness of the  $Nb_3Sn$  layer (~ 2  $\mu$ ) is such that we should have seen flux penetration through that layer to the underlying Nb if that was what was happening at the lower temperature.

It is safe to say that we do not understand the  $Nb_3Sn$  behavior at this time, but the results are quite promising for reasonably high power use of  $Nb_3Sn$  in cavities. Even though the material may show some low value of  $H_{c1}$ , the degree of flux penetration is so low at high frequencies that one may use it for reasonably high Q cavities at high power levels. It may be even more useful when the  $Nb_3Sn$  is fabricated by diffusion on Nb. This investigation is continuing, and when new funding is obtained we should be able to complete the present phase of measurements. An independent theory and modeling activity is underway to try to provide a better understanding of this behavior.

## References

1. R. V. Latham, High Voltage Vacuum Insulation, The Physical Basis, Academic Press, London/New York (1981); R. J. Noer, Appl. Phys. A28, 1 (1982).
2. R. V. Latham, "Field-Induced Electron Emission from Localized Sites on Extended-Area Electrodes," Proc. of the Second Workshop on RF-Superconductivity, H. Lengeler, Ed. (1984), pg. 533-550; Ph. Niedermann, N. Sankarraman and O. Fischer, "Investigations on Field Emission from Broad Area Nb-Cathodes," ibid, pg. 583-596.
3. S. Chamati, H. Suhl, W. Vernon and G. Webb, "Time Dependence of Magnetic Flux Penetration in Nb and Nb<sub>3</sub>Sn," IEEE Trans. Magn. MAG-21, 831 (1985).

TIME DEPENDENCE OF MAGNETIC FLUX PENETRATION IN Nb AND Nb<sub>3</sub>Sn\*

S. Ghamati, H. Suhl, W. Vernon and G. Webb  
 Department of Physics and  
 Institute for Pure and Applied Physical Sciences  
 University of California, San Diego, La Jolla, CA 92093

Abstract

We have investigated a single crystal sample of Nb<sub>3</sub>Sn at low frequencies, 100 Hz to 13 kHz, and found a value of  $B_{c1} = (45.6 \pm 2.7) \text{ mT}$  for the lower critical field extrapolated to  $T = 0 \text{ K}$  at 497 Hz. The critical field, as we have defined here, was observed to increase by  $32 \pm 5\%$  in going from 0.5 to 13 kHz. Hysteretic energy loss was used to determine the critical fields and was observed to decrease rapidly with frequency, dropping a factor of ten between 0.5 and 13 kHz. Samples of Nb wire were pulsed with field rise times of 2  $\mu\text{sec}$  and found to have a  $T = 0 \text{ K}$  value of  $B_{c1} = 158 \pm 8 \text{ mT}$ , unchanged from lower frequency values. The Nb<sub>3</sub>Sn sample had undetectable signal levels under similar pulse conditions (up to 150 mT maximum field). Temperature dependence of the critical fields is consistent with  $1 - (T/T_c)^2$  behavior from 2 K to  $T_c$  (18.0  $\pm$  0.1 K for the Nb<sub>3</sub>Sn sample).

Introduction

Superconducting cavities used for high power RF energy storage or for particle accelerators have evolved slowly in the last two decades<sup>1</sup> with niobium still the material of choice for working devices. Considerable effort has gone into the fabrication of Nb<sub>3</sub>Sn cavities because of that material's higher critical temperature and potentially higher critical magnetic field capability in comparison with Nb. However, no Nb<sub>3</sub>Sn cavities to date have significantly outperformed those fabricated from pure Nb. Since it appears that much more work will be required before high quality large area Nb<sub>3</sub>Sn surfaces can be constructed, we have begun a study of the time dependent high magnetic field behavior of a small sample of single crystal Nb<sub>3</sub>Sn.

A key uncertainty in Nb<sub>3</sub>Sn high frequency behavior comes from its rather low critical field,  $B_{c1}$ , at low frequencies. The 4.2 K value of  $B_{c1}$  at low frequencies doesn't seem to be well known either,<sup>2</sup> partly due to the difficulty in fabricating samples and partly from the complicated behavior of this material. There are calculations<sup>3</sup> which show that the Meissner state is metastable up to a higher critical field  $B_{GH}$  and that this critical field may be near or even above the thermodynamic  $B_c$  of type II materials. It has also been suggested that this metastable state may be more easily observed with RF due to a finite nucleation time for a flux line.<sup>1</sup> Since the highest fields achieved to date in Nb<sub>3</sub>Sn cavities are less than 0.1 T,<sup>4</sup> it seemed appropriate to try to find the value of  $B_{GH}$  and its low frequency onset for both Nb and Nb<sub>3</sub>Sn in small samples of very pure material.

The Apparatus

Superconducting samples were wrapped with a "sample coil" and placed in a time varying magnetic field next to a field monitoring coil so that a reasonably uniform magnetic field ( $B_a$ ) was seen by the sample and the monitor coil. Ferrite<sup>5</sup> was used to make an approximately toroidal geometry with a 1 cm<sup>2</sup> cross-section and a gap of length 2.86 mm where the sample and coils reside. The field monitor coil generates voltage  $V_a$  and consists of 30 turns of #48 Cu wire with an effective area of 1.2 mm<sup>2</sup>  $\pm$  2%, located below the gap centerline. A sample and its coil was placed above the center of the gap with center to center spacings of the coils being typically 3 mm. The magnetic field in the gap at room temperature was uniform to within 2% over the area occupied by the two coils and was generated by a winding of between 20 and 40 turns on the far leg of the toroid.

At LHe temperatures the toroid required an excitation of about 250 A-turn for 100 mT (1 kGauss) in the gap with drive voltages as high as 1000 V for the shortest time scales reported here. Magnetic fields of up to 0.15 T can be achieved with this material and winding geometry at 4.2 K before serious distortion arises due to saturation in the ferrite. The ferrite does exhibit strange low temperature behavior, but certain combinations of temperature, frequency and amplitude exist where low distortion sinusoidal time dependent fields may be generated.

Measuring the magnetic flux in the sample consisted of subtracting some fraction of  $V_a$  from  $V_s$ , the sample coil voltage, in order to create  $V_{diff} \propto d\phi_s/dt$ , the rate of change of the flux inside the sample. A network with some small phase shifting capability was used in conjunction with a variable bandwidth, variable gain difference amplifier to perform the subtraction. Adjustment of the network was done when the sample was superconducting and at magnetic field levels below  $B_{c1}$ . The network was tuned until  $V_{diff} \approx 0$ , often to a signal level of  $\leq 10 \mu\text{V}$ , rms. Effective sample area was determined from the settings of the networks and the voltage ratios of the two coils at temperatures above  $T_c$  and at low frequencies where normal state conductivity of the sample did not influence the level of flux through the sample.

A waveform digitizer was used to record the transient  $V_{diff}$  signal for subsequent storage on a computer disk file. If excessive noise was present, waveforms from several pulses were averaged. The pulse length for a given configuration was kept below 100 msec to prevent heating of the sample due to losses in the sample and in the toroid at high peak magnetic fields. Applied magnetic field  $B_a$  was obtained by integrating  $V_a$  which had either been digitized and summed in the computer or fed through an analog integrator and digitized; often both paths were recorded.

\* Supported by Office of Naval Research Contract N00014-82-K-0578.

Manuscript received September 10, 1984.

### Nb<sub>3</sub>Sn Results

A single crystal of Nb<sub>3</sub>Sn with an "arrowhead" shape and maximum dimensions of  $2.7 \pm 0.1$  mm,  $1.9 \pm 0.1$  mm and  $0.75 \pm 0.05$  mm was wound with a sample coil of 30 turns of #48 Cu wire having an effective coil area of  $0.93 \text{ mm}^2 \pm 3\%$ . The effective area of the sample perpendicular to the magnetic field was found to be  $A_s = 0.58 \text{ mm}^2 \pm 5\%$ , i. e., 63% of the sample coil area. A direct check of the critical temperature of the sample in our apparatus at very low applied field gave  $T_c = 18.0 \pm 0.1$  K.

The sample is the same single crystal used in earlier Raman scattering experiments,<sup>6</sup> where its preparation was described. Surface treatment of the sample for the Raman measurement is described elsewhere.<sup>7</sup> For this experiment the crystal axes were at unknown orientation, but with the longest dimension parallel to the applied field. Other samples from the same growth were measured to have  $T_c = 18.0$  K with residual resistance ratio (RRR) extrapolated to 0 K of 50. This RRR corresponds to a residual resistivity of  $1.5 \mu\Omega\text{cm}$ . Clear signs of a martensitic transformation at 50.6 K were observed in the resistance.

Early attempts to measure flux penetration in the sample with pulsed fields of  $\mu\text{sec}$  rise time were inconclusive. At lower frequencies some semblance of order emerged, and the results presented here come from runs at 100 Hz, 497 Hz and 13 kHz. In Fig. 1 the  $V_{\text{diff}}$  and  $V_a$  signals vs time are shown for a typical set of conditions where the signals are clean enough to do the subsequent hysteresis analysis of energy loss per cycle as  $B_a$  increases. It can be seen that  $V_{\text{diff}}$  is essentially zero until some field level where the signal begins to grow as  $B_a$  continues to increase. The shape of the  $V_{\text{diff}}$  signal provides no obvious clues about the value of  $B_{c1}$ . For instance, one might expect that a sharp spike would appear at the instant when  $B_a$  exceeds  $B_{c1}$ , as in the case for Nb samples in similar circumstances. Since the critical field for Nb<sub>3</sub>Sn cannot be determined easily by inspection, we chose to follow the energy loss per cycle as a means of defining  $B_{c1}$  with some precision.

When the voltages of Fig. 1 are integrated, the resulting time dependent magnet field flux of the sample and the applied field may be plotted as hysteresis curves as shown in Fig. 2. The vertical axis represents flux through the sample, but the right-side scale also shows a magnetic field which would correspond to that flux if the field in the sample were uniform. The two families of hysteresis loops span the region of Fig. 1(a) corresponding to positive energy loss, and the starting points of each family are shown by the arrows in Fig. 1(a). An expanded scale is used to show the loops in Fig. 2(a) where  $B_{c1}$  is found to have been reached by the increasing amplitude of  $B_a$ . Cycles earlier than the ones plotted have very small negative areas, but the noise and systematic uncertainties in the apparatus prevent us from attaching much significance to the "reversal of the sense of the loop" in this data.

Energy density lost in the sample due to flux moving in and out may be found by integrating  $(\partial_s/A_s)(dB_a/u_0)$  (or  $B_s d\partial_s/u_0$ ) for each cycle of  $B_a$ , starting at  $B_a = 0$ . This loop area is positive when the

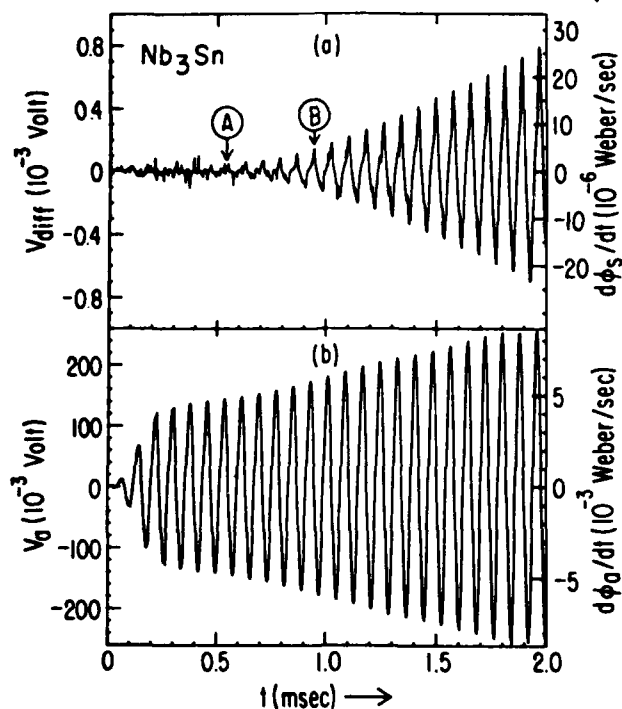


Figure 1. Sample coil voltage which is associated with the sample area (a) and applied magnetic field monitor voltage (b) for Nb<sub>3</sub>Sn at 4.2 K and 13 kHz. The time indicated by A is near  $B_a(\text{max}) = B_{c1}$  and is the start of the loops in Figure 2(a) while point B is the start of loops in Figure 2(b).

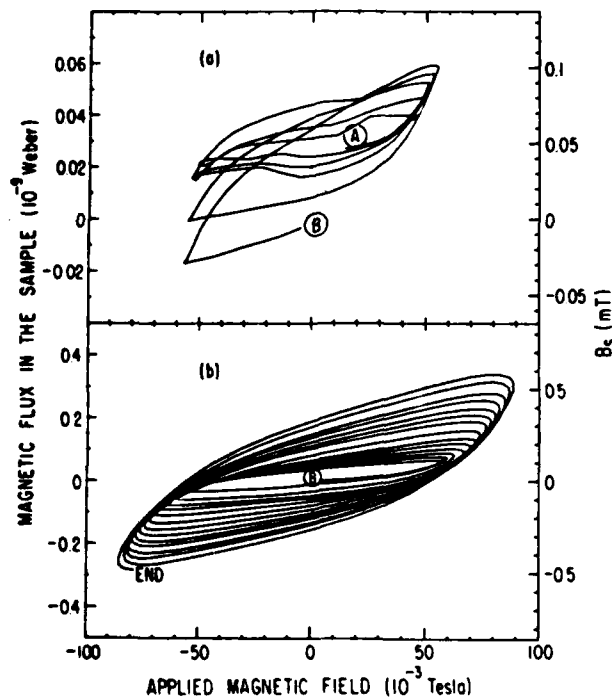


Figure 2.  $\phi_s$  vs  $B_a$  hysteresis loops for the data of Figure 1, starting at time A in (a) and continuing in (b). The right side axis shows sample field values for scale only.

loop is traversed in a counter-clockwise sense as time increases. When this energy density is multiplied by  $A_s l$ ,  $l$  the effective sample length, we arrive at an approximate energy loss per cycle for the sample. Picking  $l = 2.5$  mm as a reasonable effective length for this sample shape, we plot the energy loss/cycle as a function of the amplitude of  $B_a$  for various frequency and temperature combinations in Fig. 3. Since  $\Delta E$  is changing rapidly with both temperature and frequency, data is multiplied by various factors before being plotted in the figure.

When a quadratic function of  $B_a$  is fit to a set of energy loss points, we assume that the minimum of the function indicates where  $B_{c1}$  occurs. Three of the quadratic fits are shown in Fig. 3, and values for the quadratic parameters for all five sets are listed in Table I. The quality of the fits is consistent with statistical errors of about 5% on each point.

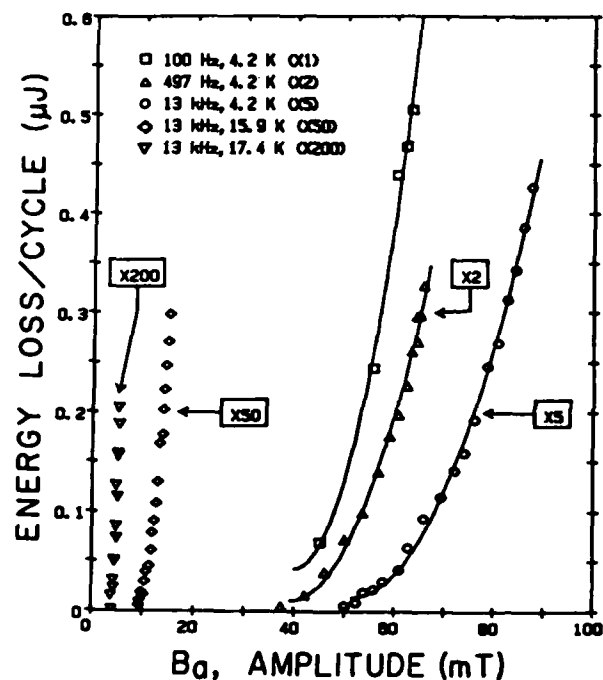


Figure 3.  $\Delta E$  vs applied magnetic field, obtained from hysteresis loop areas. The solid lines are quadratic fits whose starting points are taken to be  $B_{c1}$  for each data set. Each set has been multiplied by a different scale factor to facilitate shape comparisons.

TABLE I: Parameters in the quadratic fits of energy loss/cycle ( $\Delta E$ ) as a function of amplitude of the applied magnetic field  $B_a$  for the five cases plotted in Fig. 3. The function is  $\Delta E = E_0 + U(B_a - B_c)^2$ .

| CASE           | $E_0$ (nJ)    | $U$ (nJ/(mT) <sup>2</sup> ) | $B_c$ (mT)     |
|----------------|---------------|-----------------------------|----------------|
| 100 Hz, 4.2 K  | $43 \pm 73$   | $0.9 \pm 0.5$               | $40 \pm 7$     |
| 497 Hz, 4.2 K  | $5.4 \pm 3.8$ | $0.21 \pm 0.02$             | $39.1 \pm 1.5$ |
| 13 kHz, 4.2 K  | $2.8 \pm 0.9$ | $0.063 \pm 0.004$           | $51.6 \pm 1.0$ |
| 13 kHz, 15.9 K | $0.2 \pm 0.1$ | $0.17 \pm 0.02$             | $9.2 \pm 0.3$  |
| 13 kHz, 17.4 K | $0.0 \pm 0.1$ | $0.3 \pm 0.1$               | $3.6 \pm 0.4$  |

Temperature dependence of the critical field at a given frequency is expected to closely follow the  $B_{c1}(1 - (T/T_c)^2)$  rule which appears to be the case for the 13 kHz points. The fit results for  $B_{c1}$  are shown in Table II. Since  $B_{c1}$  may be changing with frequency, an effort was made to obtain  $B_{c1}$  at 500 Hz with minimum systematic errors. Variations in the ferrite properties with temperature prevent us from making the energy loss analysis over the whole temperature range. In order to see how the critical field changes with  $T$ , the critical field threshold was estimated by extrapolating the  $V_{diff}$  signal back to zero amplitude, and the results are plotted in Fig. 4. The 4.2 K point comes from Table I, the result of the energy loss analysis, and is combined with the lower precision points in the overall weighted fit to the quadratic temperature dependence. Parameters from the fit are  $B_{c1} = 38.4 \pm 1.2$  mTesla (500 Hz) and  $T_c = 18.4 \pm 0.4$  K where the critical temperature is actually  $18.0 \pm 0.1$  K so that there is reasonable agreement for the critical temperature found in this way.

A final problem with the  $Nb_3Sn$  sample stems from its shape and the question of what "demagnetizing" factor to ascribe to the sample. An estimate of the effect of the crystal shape<sup>8</sup> on the magnetic field at the superconducting surface yields a multiplier of  $1.19 \pm 0.07$ . The corrected values of  $B_{c1}$  are shown in Table I where the two sets of errors indicate first the uncertainty of the  $\Delta E$  vs  $B_a$  determination and, second, the overall uncertainty due to the demagnetizing correction which is the same for all data sets.

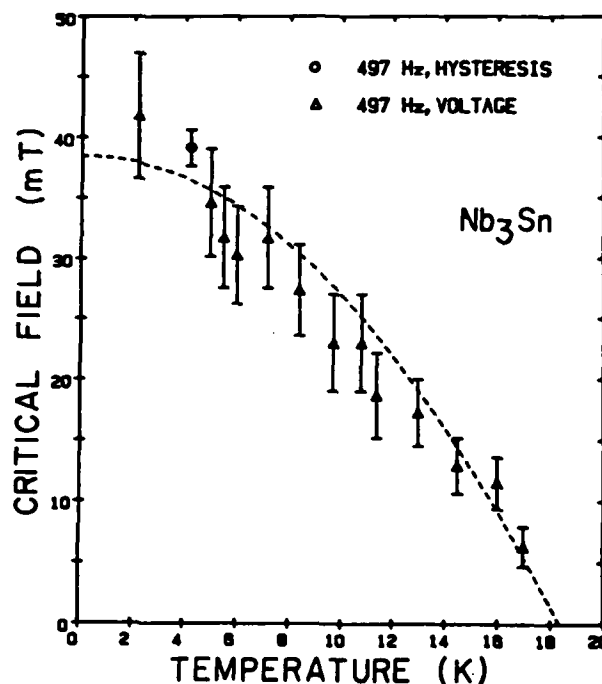


Figure 4. Temperature dependence of  $B_{c1}$  for a frequency of 497 Hz. The point at 4.2 K comes from Table I, and the remaining points are the result of extrapolation of  $V_{diff}$ . The dashed line is the fit discussed in the text.

TABLE II: The lower critical field,  $B_{c1}$ , at  $I = 0$  K as determined from fits of data to the function  $B_{c1}(0)(1 - (T/T_c)^2) = B_{c1}(T)$ . The last column is the value corrected for demagnetizing shape effects whose uncertainty is shown by the second set of errors.

| CASE                       | $B_{c1}(0)$ (mT)<br>uncorrected | $B_{c1}(0)$ (mT) |
|----------------------------|---------------------------------|------------------|
| Nb <sub>3</sub> Sn, 497 Hz | 38.4 ± 1.2                      | 45.6 ± 1.5 ± 2.3 |
| Nb <sub>3</sub> Sn, 13 kHz | 53 ± 3                          | 63 ± 4 ± 3       |
| Nb, 2μsec                  | 155 ± 8                         | 158 ± 8 ± 2      |

#### Nb Measurements

A sample of Nb wire (MRC, MARZ grade); 2.5 mm along the magnetic field direction and 0.2 mm in diameter was tested at 10 kHz and under fast rise time pulse conditions. A family of samples were annealed at 900°C for 30 min, electropolished, oxy-polished<sup>4</sup> and inspected to verify surface smoothness. The RRR of the samples was about 20 and the critical temperature was 9.14 ± 0.10 K. At 10 kHz the signal from the Nb sample coil (30 turns of #48 Cu wire) showed sharp spikes as  $B_a$  exceeded  $B_{c1}$  each half cycle. Signal strength was larger than in the Nb<sub>3</sub>Sn case even though the Nb sample area was only 1% of the Nb<sub>3</sub>Sn area.

In Fig. 5 the results of high speed pulse tests are shown for various temperatures. The increasing magnetic field had a rise time of about 2 μsec, the same for all temperatures, and was approximately bipolar (zero-integral). Critical field values were obtained by extrapolating the sample voltage waveform from its maximum slope back to the zero level. Resulting values of  $B_a$  for the five lowest temperatures were fit as shown in Table II. The fit also yielded a value of  $T_c = 9.4 ± 0.3$  K, in reasonable agreement with the known value.

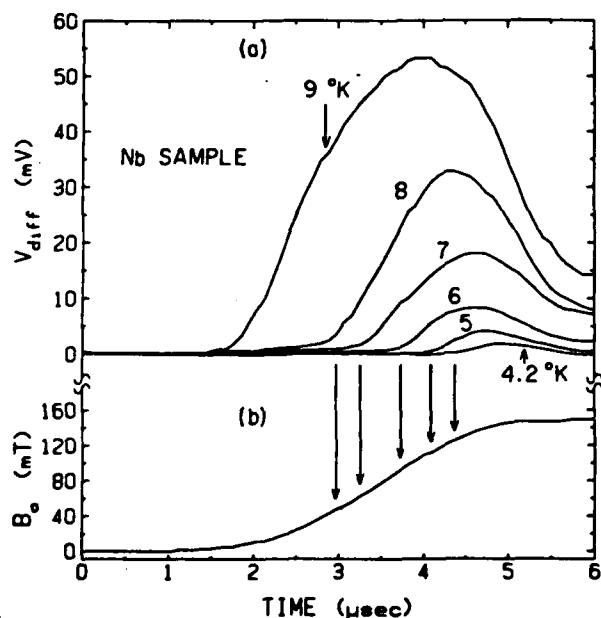


Figure 5. Nb sample voltages for several temperatures (a) and the common applied field (b). The arrows indicate the times and magnetic field values for  $B_{c1}$  with temperature decreasing to the right and arrow shown for the 9 K point.

Apart from small changes in the shape of the sample signal, there were no observed changes in  $B_{c1}$  or signal magnitudes for the frequencies covered. The shape of the signal should be changing in the μsec pulse region due to normal state conductivity restricting flux motion. Attempts to see similar signals in the pulse mode with the Nb<sub>3</sub>Sn sample were inconclusive which is understandable if the results of the previous section are extrapolated to this frequency region along with the apparatus sensitivity limits.

#### Conclusions

We have measured the lower critical field for a single crystal Nb<sub>3</sub>Sn sample at a frequency of 497 Hz by defining the start of hysteretic energy loss from our fits to the data to be the threshold. When demagnetizing corrections are included, we find  $B_{c1} = (45.6 ± 2.7) × 10^{-3}$  Tesla, extrapolated to  $T = 0$  K. Similar measurements at frequencies of 0.5 and 13 kHz and  $T = 4.2$  K indicate that the critical field, as we have defined it, increases by 32 ± 5% as the frequency is increased by a factor of 26. The energy loss per cycle,  $ΔE$ , decreases more dramatically for the same two frequencies, and the ratio of  $ΔE$  for the two cases (0.5 and 13 kHz) is about 10 in the region of  $B_a = 60$  mT. Measurements on Nb have not revealed major changes in its behavior up to equivalent frequencies of 100 kHz.

These measurements are a preliminary skirmish in the battle to characterize Nb<sub>3</sub>Sn for high frequency and high magnetic field applications. However, the results look promising and indicate that the material may have low loss applications at lower frequencies than previously considered, especially in a pulse mode which might exceed  $B_{c1}$  for short times. We will try to use that feature as a tool to create higher drive fields at higher frequencies in order to continue the study of the single crystal Nb<sub>3</sub>Sn sample.

#### Acknowledgments

We wish to thank M. Tigner for pointing out the necessity for this type of study. We also wish to thank the Institute for Pure and Applied Physical Sciences for the support given during the course of this work.

#### References

1. M. Tigner and H. Padamsee, *Physics of High Energy Particle Accelerators*, AIP Conference Proceedings Number 105, p. 801 (1983).
2. R. Shaw, B. Rosenblum and F. Bridges, *IEEE Trans. Magn.*, **MAG-13**, 811 (1977).
3. L. Kramer, *Z. Physik*, **259**, 333 (1973).
4. N. Krause, B. Hillenbrand, H. Pfister and Y. Uzel, *IEEE Trans. Magn.*, **MAG-17**, 927 (1981). Also see D. F. Moore and M. R. Beasley, *Appl. Phys. Letters* **30**, 494 (1977) who report indirect tunneling observations of delayed flux entry at d. c. in Nb<sub>3</sub>Sn films to 170 mT.
5. Fair-Rite Corp., Type 72 material.
6. S. B. Dierker, M. V. Klein, G. W. Webb and Z. Fisk, *Phys. Rev. Letters* **50**, 853 (1983).
7. S. B. Dierker, Thesis, University of Illinois (unpublished).
8. J. A. Osborn, *Phys. Rev.* **67**, 351 (1945).

**END**

**FILMED**

---

*1-86*

**DTIC**